Agr. Nat. Resour. 56 (2022) 713–724

AGRICULTURE AND NATURAL RESOURCES

Journal homepage: http://anres.kasetsart.org

Research article

Combining high-throughput phenotyping with overall growth measurements of indica rice (*Oryza sativa* L spp. *indica*) cultivars over the whole life cycle

Cattarin Theerawitaya[a], Cattleya Chutteang[b,*], Anuruck Arunyanark[b], Chanate Malumpong[b], Narubodin Kwangern[b], Nattapol Rachsapa[b], Piyanan Pipatsitee[a], Patchara Prasertkul[a], Suriyan Cha-um[a], Theerayut Toojinda[a]

[a] *National Center for Genetic Engineering and Biotechnology (BIOTEC), National Science and Technology Development Agency (NSTDA), Pathum Thani 12120, Thailand*

[b] *Department of Agronomy, Faculty of Agriculture at Kamphaeng Saen, Kasetsart University, Nakhon Pathom 73140 Thailand*

Article Info

Article history:
Received 6 October 2021
Revised 15 May 2022
Accepted 20 May 2022
Available online 26 August 2022

Keywords:
Canopy height,
High-throughput phenotyping,
Oryza sativa,
Plant projected area,
Red-green-blue (RGB)

Abstract

Importance of the work: High-throughput phenotyping systems containing non-destructive and non-invasive characterizations of phenotypic traits throughout the whole life cycle of plant development have prevailed over the conventional method.

Objectives: To evaluate the phenotypic characteristics of indica rice genotypes using red-green-blue (RGB) high-throughput phenotyping over the whole life cycle in relation to biomass and yield components.

Materials & Methods: Plant canopy width, canopy height and leaf area values of the rice cultivars RD41, Pathumthani1 (PT1), Homchonlasit, IR64, Riceberry and RD43 were measured using RGB imagery estimation together with actual measurements at 45 d after planting (DAP), 60 DAP, 75 DAP, 90 DAP, 105 DAP and 120 DAP.

Results: Canopy width and canopy height values obtained from actual measurements were linearly related to RGB-estimated values in all rice cultivars with values for the correlation coefficient (r) of 0.87–0.93 and 0.90–0.99, respectively. Notably, there was a positive relationship between plant projected area from the RGB imagery and the leaf area measurement, especially at the vegetative stage (r = 0.93–0.99). At harvest, there was also a positive relationship between aboveground biomass and total yield (coefficient of determination (R^2) = 0.44). The agronomical traits and plant characterizations of RD41, PT1, Homchonlasit, IR64, Riceberry and RD43 were validated over the whole life cycle of rice crops.

Main finding: High-throughput phenotyping data collection should overcome conventional measurements due to its non-destructive, rapid and automated production for large amounts of data and high accuracy in indica rice crops.

* Corresponding author.
E-mail address: agrcyc@ku.ac.th (C. Chutteang)

https://doi.org/10.34044/j.anres.2022.56.4.06

Introduction

Rice crops are a staple food that provides carbohydrate sources for more than one-half of the world's population, especially people living in Asia (Khush, 2005). Rice grain consumption in Europe, Australia, North America and Latin America has continually increased (Muthayya et al., 2014; Firdaus et al., 2020). Efficient production strategies, including plant breeding programs, suitable cultivation and effective agricultural management using modern technology, are required to improve rice yields to meet the demand for food resources (Chawade et al., 2018). Consequently, modern idiotypes of rice crops based on stay-green and erect leaves, high photosynthetic abilities, highly efficient sink-source relationships and deep root traits have played a key role in domesticating rice to enhance its yield traits (Peng et al., 2008; Dingkuhn et al., 2015; Liang et al., 2017; Haghshenas et al., 2020). Phenotypic characteristics in rice crops fluctuate depending on genotypic variations and environmental cues (genotype by environment interaction; G×E interaction) throughout the whole life cycle (Dhondt et al., 2013; Zhang et al., 2017a; Omari et al., 2020). In rice phenotyping, canopy height, canopy width and leaf area index are the basic agronomical parameters that have indicated the aboveground biomass and predicted grain yield (He et al., 2019; Li et al., 2019). A close relationship between the total leaf area and biomass of rice crops at different growth stages has been demonstrated (Zhang et al., 2014; Lee et al., 2018). Rice biomass has also been extensively evaluated to assess plant growth status and predict grain yield (Zheng et al., 2019). Thus, achieving the basic measurement of individual quantitative parameters is a promising way to assess valuable data for the further study of complex traits (Li et al., 2014). However, traditional ways of estimating rice phenotyping traits are weak, time consuming, labor intensive, potentially damaging (destructive measurement) and prone to errors (Jiang and Li, 2020). Furthermore, the expression of each rice genotype changes and varies along the different stages of the life cycle (Li et al., 2014). Monitoring rice phenotypes that change throughout their life cycle increases the throughput and difficulty for plant researchers. Therefore, high-throughput strategies are necessary to increase the efficiency of the phenotyping measurement process (Yang et al., 2013; Araus and Cairns, 2014; Mir et al., 2019; Kim et al., 2020; Yang et al., 2020).

High-throughput phenotyping systems with the ability to perform nondestructive and noninvasive characterizations for phenotypic traits with high efficiency, great precision and automation have been well established to monitor the adaptive abilities of higher plants throughout the whole lifecycle across crop seasons (Li et al., 2014; Fahlgren et al., 2015b; Großkinsky et al., 2015). In addition, continuing advances in high-resolution imaging systems, computing capacity and image processing algorithms offer great opportunities to develop non-destructive high-throughput methods (Klukas et al., 2014; Wang et al., 2020). An affordable means has been reported of assessing genotypic differences in cereal crops using vegetation indices derived from RGB (red-green-blue) imagery (Fiorani and Schurr, 2013; Araus et al., 2018). High-throughput phenotyping technology is effectively assessed to measure the overall growth characteristics over the whole life cycle of rice crops. In the indica subtype of rice, there is still a lack of important information on high-throughput phenotyping, especially regarding associated traits related to grain yield. To date, there is limited information on the diversity of leaf color in rice crops, including light green, dark green, purple and pink colors, detected by RGB cameras via high-throughput phenotyping in relation to plant canopy estimation and color segmentation as an alternative information source (Peng et al., 2006; Chin et al., 2016; Khan et al., 2020). Riceberry is a previously documented indica rice variety with a purple leaf sheath (anthocyanin enrichment in the leaf sheath, panicle and pericarp of rice grain) (Daiponmak et al., 2010; Phonsakhan and Kong-Ngern, 2015). Additionally, in the current study rice varieties with light green, green and dark green leaves and short-day photoperiod insensitivity were selected—Homchonlasit, IR64, PT1, RD41, and RD43—as well as a semidwarf rice with a high-yield genotype, IR64, for validation (Mackill and Khush, 2018; Pongprayoon et al., 2019; Tisarum et al., 2019). There is a lack of basic information on high-throughput phenotyping of key features of elite genotypes of indica rice that are dominant in irrigated paddy fields in the central plain region of Thailand, which is the main area of rice production in the country (Office of Agricultural Economics, 2021). The objective of this experiment was to evaluate the phenotypic characteristics using RGB high-throughput phenotyping over the whole life cycle of rice.

Materials and Methods

Plant materials and culture conditions

Rice seeds from the cultivars RD41, Pathumthani1 (PT1), Homchonlasit, IR64, Riceberry and RD43 provided by the

Rice Gene Discovery Unit, National Center for Genetic Engineering and Biotechnology (BIOTEC), National Science and Technology Development Agency (NSTDA) were sown in the soil substrate for the germination process. After 2 wk, seedlings containing 2–3 leaves (shoot height 5–10 cm) were collected and subsequently transplanted into 20 cm diameter plastic pots containing commercial soil (EC = 1.687 dS/m; pH = 5.5; organic matter = 10.36%; total N = 0.17%; total P = 0.07%; total K = 1.19%). Fertilizer (16-16-16 for N-P-K) at 2 g per pot was applied monthly. The plants were grown at the Plant Phenomics Center, Rice Science Center & Rice Gene Discovery Unit, Kasetsart University Kamphaeng Saen Campus, Nakhon Pathom, Thailand. A good level of irrigation (5 cm flooding with water) was supplied to each pot. Greenhouse conditions were set at 80–90% relative humidity, a 500–800 $\mu mol/m^2/s^1$ photosynthetic photon flux density light intensity under natural sunlight and the air temperature was controlled at 35±2°C during the day and 28±2°C at night.

Red-green-blue image capture and extraction of image-based parameters

Rice plants were photographed using a PlantScreen™ RGB Imaging Unit at 2,650 pixels × 1920 pixels resolution (Photon Systems Instruments, spol.s r.o.; Czech Republic). The GigE eEye UI-5580SE-C-5 pixel QSXGA cameras with ½" CMOS sensors (Aptina Imaging Corporation; USA) were equipped at a side position in the imaging unit. For the side view camera, linear scanning mode was used and measured 1,030 mm × 1,400 mm (height × width dimensions). Two images were taken of each plant at 0° and 90° rotation. After obtaining the RGB images, the captured images were analyzed using the PlantScreen™ data analyzer software. The background was subtracted from the plant images and the noise was reduced. The canopy width, canopy height, plant projected area and perimeter were the image-based parameters that were estimated. The perimeter was defined as the length of the outside boundary of the object (Kim et al., 2020). The plant volume was calculated according to Arend et al. (2016) using Equation 1:

$$V = \sqrt{At \times A0° \times A90°} \quad (1)$$

where V is the volume of the plant (in cubic centimeters), At is the computed top area (in square centimeters), A0° is the computed side area at 0° (in square centimeters) and A90° is the computed side area at 90 (in square centimeters).

Color segmentation was provided using nine shades of color. Yellow and green colors were dissected as yellow (110; 111; 90, 90; 98; 58, or 72; 84; 58) and green (73; 86; 36, 57; 71; 46, 59; 71; 20, 45; 55; 36, 45; 54; 13, or 34; 38; 22), respectively.

Data measurement of aboveground traits

Shoot height, canopy width and leaf area values in rice genotypes at 45 DAP, 60 DAP, 75 DAP, 90 DAP, 105 DAP and 120 DAP were manually measured in parallel to the RGB image capture. The shoot height of the plant was measured as the distance from the base of the plant to the tip of the tallest leaf. The canopy width of the plant was measured from one edge of the plant to the opposite edge of the plant, while allowing the plant to freely stand in the pot. The canopy width was obtained from two sides at an approximately 90° difference. Plant leaf area was determined using a leaf area meter (LI-3100 C, Li-Cor, Inc.; USA) by placing the sample leaves on the leaf area meter desktop and securing them in a flat position. In addition, the number of tillers was counted and the shoot fresh weight (FW) and shoot dry weight (DW) were determined. The shoot dry weight of the plants was obtained by drying them in a 110 °C hot-air oven for 3 d and then cooling the samples to room temperature in a desiccator. The weight of the sample was measured using a 2-digit balance.

Determination of yield components

In the harvest process, mature rice panicles that had turned yellow were subsequently harvested to determine the yield and yield components (the number of panicles per plant, number of seeds per panicle and grain fertility percentage) following Cha-um and Kirdmanee (2010). Rice panicles were dried at 45 °C for 3 d before measuring the panicle dry weight and 100-grain weight, which were determined using a 2-digit balance. The grain yield was determined from each plant and adjusted to a moisture content of 14%.

Experimental design and statistical analysis

The greenhouse experiment was laid out in a randomized complete block design with six replications (n = 6). Analysis of variance was performed for each variable. Mean comparisons of each parameter were distinguished using Tukey's honestly significant difference. Linear regression equations were calculated for the associations between variables. Simple

correlations between parameters obtained from the high-throughput system and manual measurements were also computed using the Pearson correlation coefficient (r). All tests were considered significant at $p < 0.05$. Statistical analyses were performed using the SPSS ver.11.5 (SPSS for Windows®; USA).

Results

Canopy width, canopy height and leaf area

The canopy width of each rice cultivar at different developmental stages using conventional practice was larger than that using RGB estimation. The canopy width of the rice cultivars RD41, PT1, Homchonlasit, IR64, Riceberry and RD43 continuously increased across growth periods from 45 DAP to 120 DAP (Table 1). A positive relationship between the actual measurement and RGB estimation of canopy width using Pearson's correlation coefficient was observed r = 0.58–0.81 (Table 2). There was a positive relationship between the actual measurement and RGB estimation in individual rice cultivars (r = 0.87 to r = 0.93). Therefore, canopy width measurement using the conventional method was better than that based on RGB two-shot imagery estimation (Fig. 1). For the conventional protocol, canopy height was measured from the soil surface to the tip of the tallest leaf at the vegetative or panicle stage during reproduction. In contrast, using RGB imagery, shoot height was measured from the top of pots containing plants with normal expansion of the canopy, which was shorter than that height for conventional practice. Shoot height in the rice cultivars RD41, PT1, Homchonlasit, IR64, Riceberry and RD43 increased throughout the growing period (Table 1). At the ripening stage (105–120 DAP), shoot height measurements in the cultivars PT1, Homchonlasit and IR64 declined based on the conventional method, depending on leaf tip burn and drop-down (senescence). A constant shoot height at the ripening stage of the rice cultivars PT1 and IR64 was observed using RGB imagery (Table 1). Based on Pearson's correlation coefficient, there was a close relationship between the actual values for canopy height and the RGB estimation values at each developmental stage (r = 0.77–0.98), as shown in Table 2. There was a linear relationship between the RGB estimation and actual measurement values of canopy height (r = 0.90–0.99), as shown in Fig. 2 and Table 2.

The plant projected area derived from RGB imagery was lower than that from the leaf area values obtained from the leaf area measurements (Table 1). In the vegetative stage (45–90 DAP), the leaf area continuously increased with a high correlation coefficient (r = 0.70–0.95), as shown in Table 2. In contrast, the leaf area declined at the reproductive stage, especially in RD41 and RD43 (the early harvesting genotypes), leading to fluctuations in each genotype (r = 0.38), depending on leaf chlorosis and senescence. In addition, a positive relationship was observed between the actual and RGB measurements at 120 DAP, with the data for RD41 and RD43 omitted (r = 0.70). The leaf area at the vegetative stage at each measurement based on the conventional data was linearly correlated with that for RGB estimation (r = 0.93–0.99), as shown in Fig. 3. At the reproductive stage, a positive relationship between the actual leaf area measurement and RGB estimation was only found for RD41 (r = 0.78) and Homchonlasit (r = 0.64), as shown in Fig. 3. Interestingly, color segmentation evaluation in the plant canopy of rice crops over the whole life cycle was categorized into two harvest groups: early (RD41 and RD43) and late (PT1, Homchonlasit, IR64 and Riceberry). The early harvest plants stayed green within 90 DAP as was observed for RD41, whereas leaf chlorosis or yellowing increased after 90 DAP and reached a maximum at 105 DAP for RD43 (Fig. 4). Riceberry stayed green for the entire life cycle, with purple leaf sheaths and panicles (Fig. 4E). Leaf segmentation stayed green for IR64 (Fig. 4D), depending on the breeding strategies for the high-yielding cultivar adopted by IRRI. In contrast, green leaf color segmentation in the cultivars Homchonlasit and PT1 was retained at high levels at ≤ 90 DAP, and the segments subsequently turned yellow, especially at 120 DAP, before the harvest period (Figs. 4B–4C).

Relationship between data obtained from RGB imagery and actual measurements

In the vegetative stage, there were positive relationships between perimeter and the number of tillers (Fig. 5A; coefficient of determination (R^2) = 0.32), canopy width and shoot fresh weight (Fig. 5B; $R^2 = 0.53$) and plant projected area and shoot dry weight (Fig. 5C; $R^2 = 0.93$). Those parameters in the reproductive stage had R^2 values of 0.29, 0.09 and 0.48, respectively (Figs. 5D–5F). There were positive relationships between the number of green pixels and shoot fresh weight (Fig. 6A; $R^2 = 0.31$), plant volume and shoot fresh weight (Fig. 6B; $R^2 = 0.86$), plant volume and shoot dry weight (Fig. 6C; $R^2 = 0.77$) and shoot dry weight and grain yield (Fig. 6D; $R^2 = 0.44$).

Table 1 Canopy width, canopy height and leaf area values estimated from red-green-blue (RGB) imaging unit and actually measured in rice cultivars RD41, PT1, Homchonlasit, IR64, Riceberry and RD43 over the whole life cycle of 45–120 d after planting (DAP)

Genotype	45 DAP		60 DAP		75 DAP		90 DAP		105 DAP		120 DAP	
	Actual	RGB	Actual	RGB	Actual	RGB	Actual	RGB	Actual	RGB	Actual	RGB
						Canopy width (cm)						
RD41	32.8±2.2^{abc}	17.5±1.0^{b}	40.5±1.7^{b}	28.9±1.8^{c}	51.0±2.3^{bc}	41.9±2.4	59.3±4.1^{bc}	44.5±1.3^{b}	66.8±2.5^{c}	44.9±1.4^{c}	NA	NA
PT1	36.3±1.9^{ab}	23.0±1.0^{b}	57.8±2.6^{a}	48.1±2.4^{a}	53.8±1.1^{abc}	39.8±1.3	64.2±2.6^{bc}	49.4±1.7^{ab}	80.7±4.3^{bc}	53.4±1.0^{b}	80.9±1.7^{bc}	56.1±0.7
Homchonlasit	38.5±1.8^{a}	30.1±1.7^{a}	50.2±2.1^{ab}	43.1±2.2^{ab}	58.5±0.9^{a}	42.3±0.7	83.0±7.0^{a}	55.9±2.7^{a}	99.3±4.6^{a}	59.7±0.2^{a}	103.7±4.4^{a}	54.2±2.4
IR64	29.0±2.2^{c}	19.4±2.1^{b}	50.0±3.8^{ab}	43.0±4.7^{ab}	51.5±2.5^{abc}	37.9±3.2	53.7±1.3^{c}	44.3±1.7^{b}	69.7±3.6^{c}	54.3±0.9^{b}	87.0±4.6^{b}	57.9±1.2
Riceberry	30.2±1.5^{bc}	19.9±0.9^{b}	44.0±4.4^{b}	34.1±2.9^{bc}	49.8±0.8^{c}	38.1±1.3	56.5±2.3^{c}	45.2±1.6^{b}	70.0±2.8^{c}	52.6±2.0^{b}	76.7±3.8^{c}	57.0±1.0
RD43	31.7±0.7^{bc}	19.7±1.3^{b}	51.7±2.2^{ab}	34.3±3.1^{bc}	58.2±3.8^{ab}	42.3±3.1	74.3±3.8^{ab}	54.9±1.5^{a}	89.2±6.3^{ab}	56.7±1.5^{ab}	NA	NA
F-test	**	**	**	**	**	ns	**	**	**	**	**	ns
CV (%)	11.0	14.9	13.9	15.4	7.7	11.3	13.6	8.2	12.4	5.1	5.6	5.7
						Canopy height (cm)						
RD41	32.5±1.1^{b}	27.9±1.4^{c}	49.7±1.4^{b}	49.1±1.2^{b}	72.7±2.4^{b}	72.2±2.7^{b}	95.2±3.2^{ab}	96.8±3.3^{b}	100.7±2.6^{abc}	106.7±2.4^{ab}	NA	NA
PT1	42.0±1.3^{a}	38.9±1.8^{ab}	53.0±2.2^{ab}	52.7±2.4^{b}	68.2±0.7^{bc}	68.1±1.4^{b}	89.0±1.4^{b}	87.5±3.1^{b}	114.8±2.4^{a}	113.6±1.9^{a}	109.0±2.3^{b}	114.6±1.5^{a}
Homchonlasit	44.0±2.4^{a}	44.0±1.9^{a}	53.7±1.8^{ab}	52.5±1.2^{b}	65.3±0.4^{cd}	65.2±1.3^{bc}	97.8±5.9^{ab}	94.0±5.0^{b}	98.8±7.3^{bc}	108.1±3.1^{ab}	83.8±3.5^{c}	88.1±2.0^{b}
IR64	38.2±2.1^{ab}	36.8±2.1^{b}	46.0±0.8^{b}	47.3±1.1^{b}	55.7±1.7^{e}	54.2±1.3^{d}	74.0±2.6^{c}	74.9±2.3^{c}	85.7±4.3^{c}	89.8±1.0^{c}	77.4±5.2^{c}	80.2±3.7^{c}
Riceberry	32.3±0.9^{b}	33.0±0.8^{bc}	49.7±2.9^{b}	47.1±2.8^{b}	61.3±1.9^{de}	59.2±1.5^{cd}	87.7±1.6^{b}	87.7±1.8^{b}	110.7±2.3^{ab}	112.6±1.5^{a}	125.2±0.9^{a}	116.5±0.2^{a}
RD43	33.8±2.7^{b}	29.2±0.7^{c}	60.2±2.0^{a}	62.2±1.4^{a}	88.3±3.5^{a}	87.1±3.4^{a}	105.0±1.4^{a}	111.0±1.4^{a}	95.8±4.4^{bc}	101.0±4.6^{b}	NA	NA
F-test	**	**	**	**	**	**	**	**	**	**	**	**
CV (%)	11.1	9.5	8.4	8.0	5.1	5.8	7.4	6.8	8.8	4.8	6.9	4.4
						Leaf area (cm^2)						
RD41	112.7±10.0^{bc}	30.4±2.9^{b}	353.5±36.6^{b}	166.5±16.2^{b}	1047.8±48.9	461.6±22.6^{bc}	1016.7±145.2^{bc}	609.4±46.1^{c}	831.7±48.0^{bc}	625.1±26.5^{b}	NA	NA
PT1	204.5±22.8^{a}	73.2±3.8^{a}	932.5±102.1^{a}	388.2±42.3^{a}	1284.3±97.7	565.5±22.6^{a}	2160.3±246.2^{a}	1053.6±118.3^{a}	1014.5±87.3^{b}	866.3±25.6^{a}	1118.8±84.4^{ab}	1233.0±77.1^{a}
Homchonlasit	168.1±15.5^{ab}	65.6±6.9^{a}	495.0±63.0^{b}	240.9±30.2^{b}	1038.0±58.6	461.0±16.6^{bc}	1473.7±219.6^{bc}	857.6±85.5^{abc}	826.0±44.4^{bc}	922.6±90.0^{a}	441.3±106.7^{c}	626.6±69.2^{c}
IR64	202.1±19.4^{a}	73.8±8.2^{a}	967.0±130.0^{a}	398.1±51.1^{a}	1236.2±63.3	531.4±23.9^{ab}	1469.0±121.4^{bc}	951.0±74.0^{ab}	789.8±49.3^{bc}	919.2±30.5^{a}	754.4±52.5^{bc}	644.4±86.6^{c}
Riceberry	157.4±8.0^{abc}	44.3±2.2^{b}	475.8±77.2^{b}	170.3±28.8^{b}	988.6±55.1	398.0±18.1^{c}	1561.0±99.7^{b}	741.5±25.2^{bc}	1385.0±91.0^{a}	957.1±71.9^{a}	1258.6±188.6^{a}	981.7±76.6^{b}
RD43	104.0±11.6^{c}	30.3±4.0^{b}	511.8±68.0^{b}	224.3±31.7^{b}	1230.8±187.4	536.3±40.8^{ab}	986.0±66.8^{c}	700.4±36.0^{bc}	694.4±72.1^{c}	607.7±46.3^{b}	NA	NA
F-test	**	**	**	**	ns	**	**	**	**	**	**	**
CV (%)	22.4	21.8	32.1	27.7	17.1	11.2	22.0	20.2	17.3	14.2	30.6	15.2

DAP = days after planting; Different lowercase superscripts in each column represent significant differences ($p < 0.05$). NA = data not available due to early harvesting; ns = not significant ($p < 0.05$); ** = highly significant ($p < 0.01$)

Table 2 Correlation coefficients (r) of canopy width, canopy height and leaf area values estimated from red-green-blue imaging unit and actually measured in six rice cultivars at 45–120 d after planting (DAP)

	45 DAP (n = 36)	60 DAP (n = 36)	75 DAP (n = 36)	90 DAP (n = 36)	105 DAP (n = 36)	120 DAP (n = 24)	Over all (n = 204)
Canopy width	0.58**	0.79**	0.68**	0.81**	0.58**	-0.22	0.87**
Canopy height	0.77**	0.87**	0.98**	0.93**	0.80**	0.95**	0.98**
Leaf area	0.91**	0.95**	0.70**	0.83**	0.38*	0.70**	0.76**

DAP = days after planting; * = significant ($p < 0.05$); ** = highly significant ($p < 0.01$)

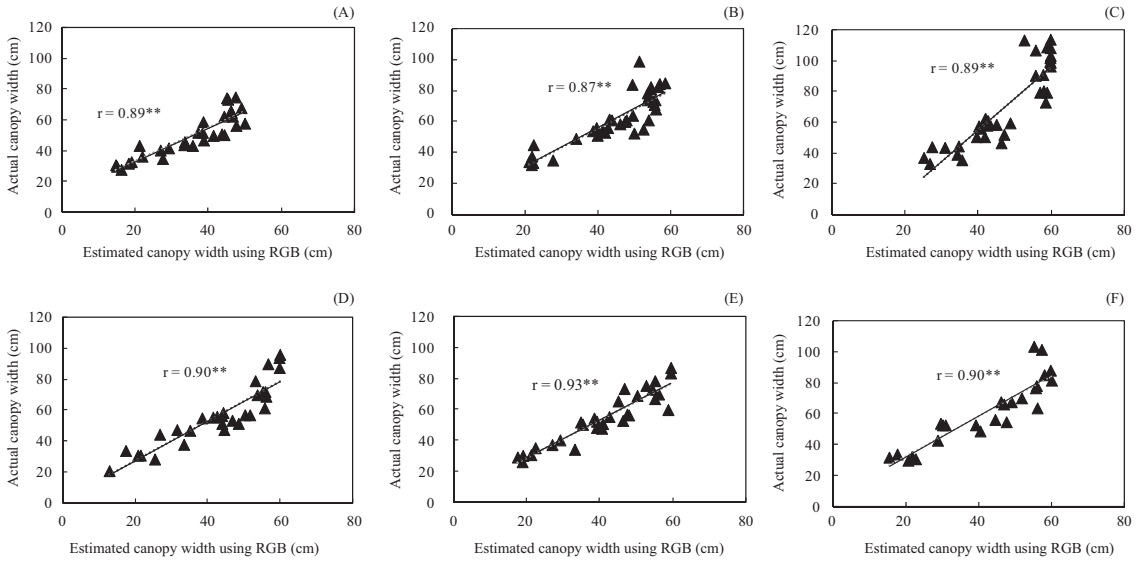

Fig. 1 Relationships between actual canopy width and estimated canopy width using red-green-blue (RGB) imagery in indica rice genotypes grown in an automatic cultivated greenhouse: (A) RD41; (B) PT1; (C) Homchonlasit; (D) IR64; (E) Riceberry; (F) RD43, where number of days after planting are indicated in Table 2 and ** = highly significant ($p < 0.01$)

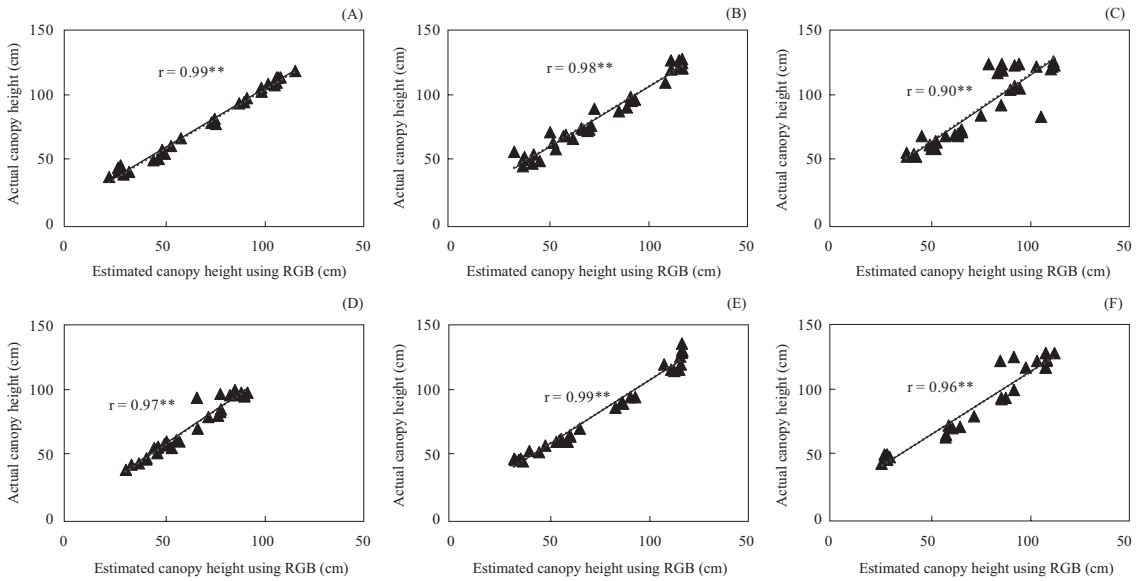

Fig. 2 Relationships between actual canopy height and estimated canopy height using red-green-blue (RGB) imagery in indica rice genotypes grown in automatic cultivated greenhouse: (A) RD41; (B) PT1; (C) Homchonlasit; (D) IR64; (E) Riceberry; (F) RD43, where number of days after planting are indicated in Table 2 and ** = highly significant ($p < 0.01$)

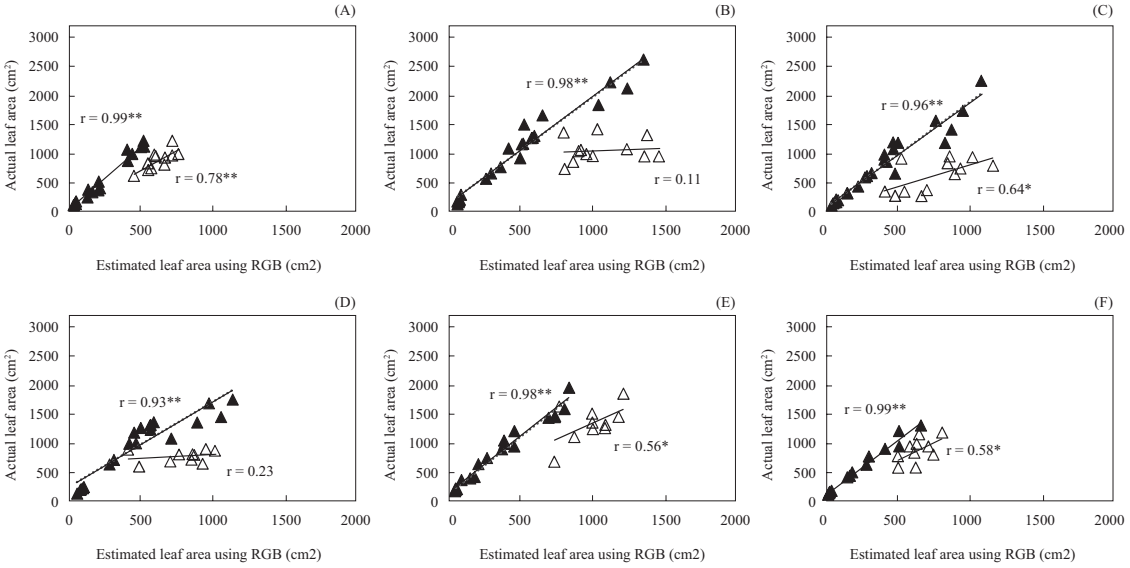

Fig. 3 Relationships between actual leaf area and estimated leaf area using red-green-blue (RGB) imagery in indica rice genotypes grown in automatic cultivated greenhouse: (A) RD41; (B) PT1; (C) Homchonlasit; (D) IR64; (E) Riceberry; (F) RD43, where data were separated into two groups, with group one obtained from vegetative stage (filled triangles) and reproductive stage (unfilled triangles); ns = non-significant ($p \geq 0.05$); * = significant ($p < 0.05$); ** = ($p < 0.01$)

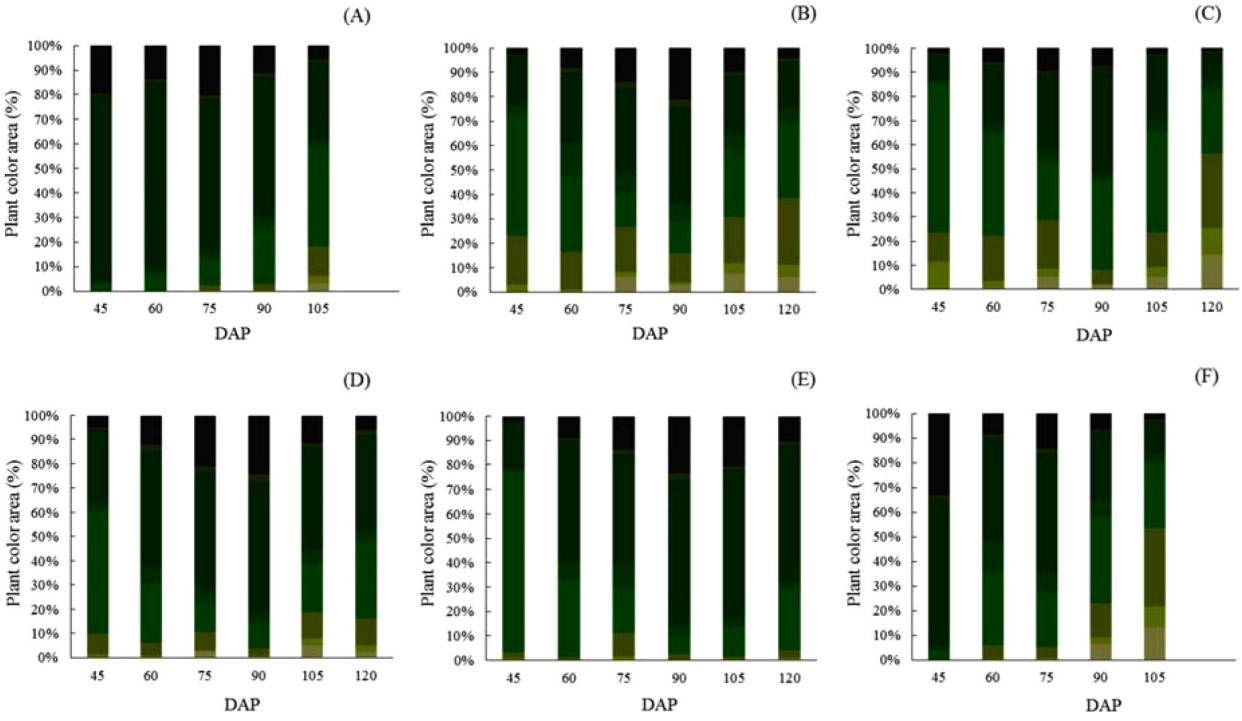

Fig. 4 Color segmentation derived from red-green-blue imagery in indica rice genotypes grown in automatic cultivated greenhouse: (A) RD41; (B) PT1; (C) Homchonlasit; (D) IR64; (E) Riceberry; (F) RD43, where DAP = days after planting

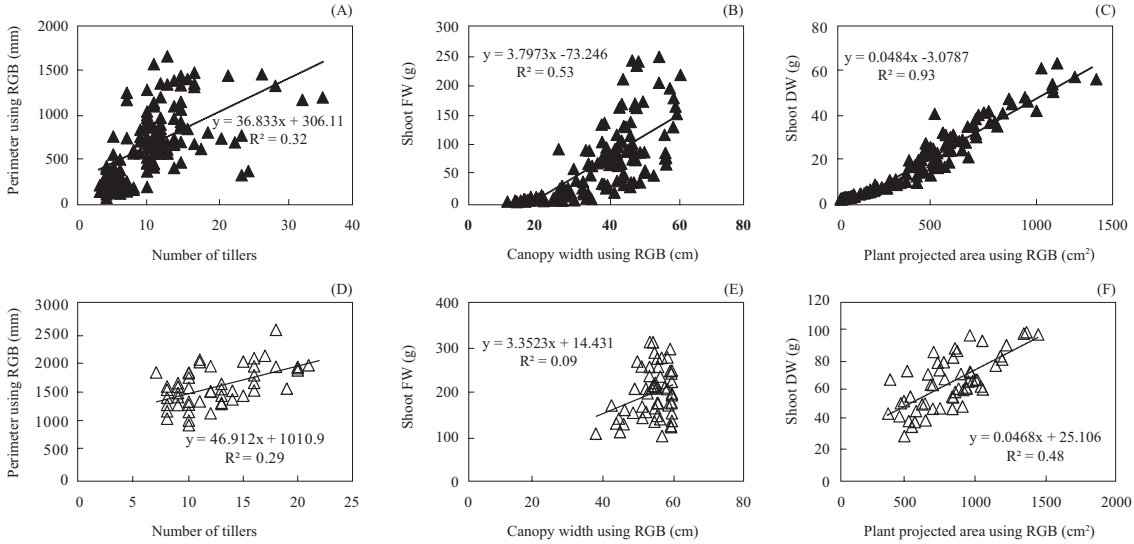

Fig. 5 Relationships of six rice genotypes grown in automatic cultivated greenhouse between: (A) number of tillers and perimeter using red-green-blue (RGB) imagery; (B) canopy width and shoot fresh weight; (C) plant projected area and shoot dry weight at vegetative stage; (D) number of tillers and perimeter using RGB imagery; (E) canopy width and shoot fresh weight (FW); (F) plant projected area and shoot dry weight (DW), where R^2 = coefficient of determination

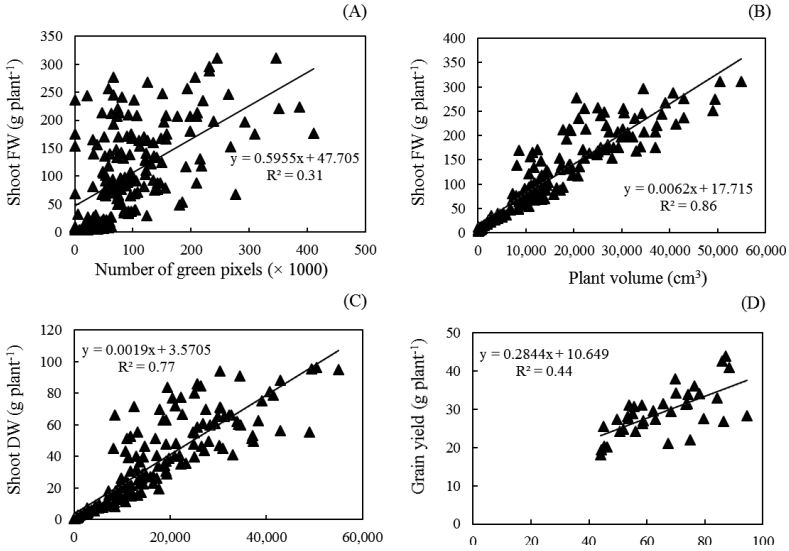

Fig. 6 Relationships of six rice genotypes grown in automatic cultivated greenhouse between: (A) number of green pixels and shoot fresh weight (FW); (B) plant volume and shoot fresh weight; (C) plant volume and shoot dry weight (DW); (D) shoot DW and total grain yield per plant

Overall growth performances and yield components

The agronomic traits and yield components of RD41, PT1, Homchonlasit, IR64, Riceberry and RD43 were measured at the harvesting stage. The number of tillers was the highest for Riceberry and the lowest for IR64. (Fig. 7A). The shoot fresh weights of PT1 and Riceberry were higher than those of other cultivars (Fig. 7B). The shoot dry weights and leaf dry weights of PT1, Homchonlasit and Riceberry were significantly higher than for the other cultivars (Figs. 7C–7D). In addition, the stem dry weights and root dry weights of Riceberry were the highest across the measured biomass traits (Figs. 7E–7F). Of the yield components, the panicle number (Fig. 8A), number of seeds per panicle (Fig. 8B) and panicle weight (Fig. 8D) of Homchonlasit were the highest, leading to its maximal total yield per plant (Fig. 8F). The grain fertility of IR64 was higher than for Riceberry by 1.5-fold (Fig. 8C), and the 100-grain weight of RD43 was the highest and was greater than that of Riceberry by 1.58-fold (Fig. 8E).

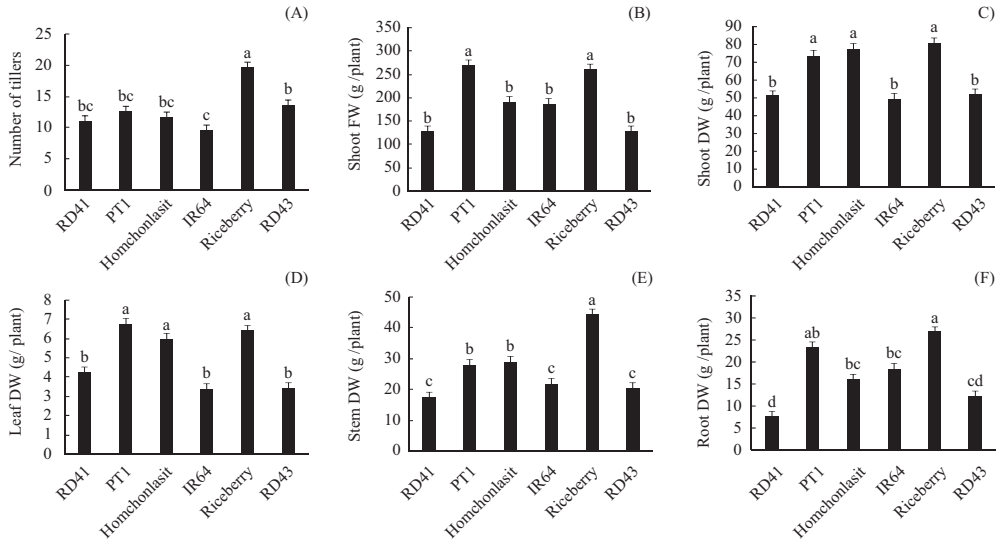

Fig. 7 Comparisons between six rice genotypes grown in automatic cultivated greenhouse for: (A) number of tillers; (B) shoot fresh weight (FW); (C) shoot dry weight (DW); (D) leaf DW; (E) stem DW; (F) root DW, where different lowercase letters above bars represent significant differences ($p < 0.05$); error bars = ±SD

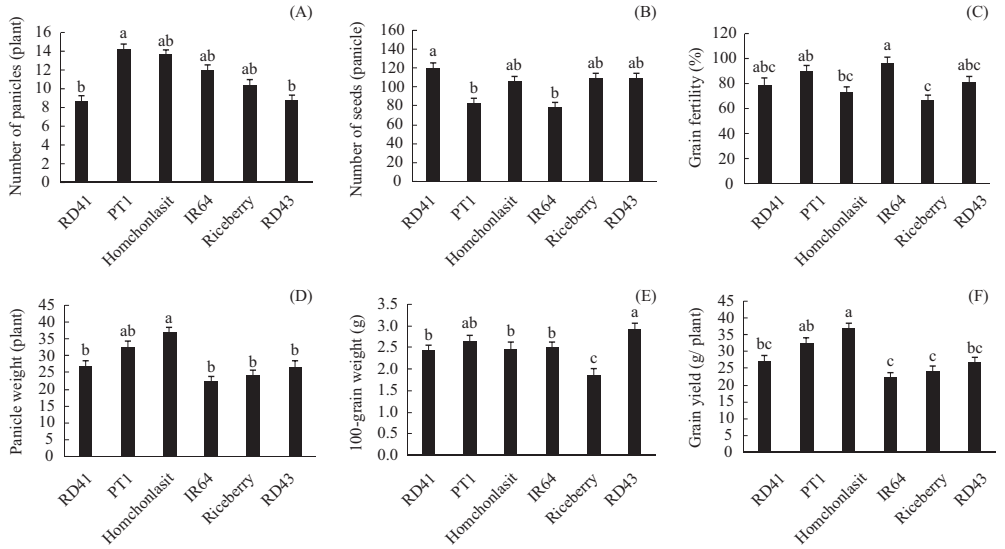

Fig. 8 Comparisons between six rice genotypes grown in automatic cultivated greenhouse for: (A) number of panicles per plant; (B) number of seeds per panicle; (C) grain fertility percentage; (D) panicle weight; (E) 100-grain weight; (F) grain yield per plant (F), where different lowercase letters above bars represent significant differences ($p < 0.05$); error bars = ±SD

Discussion

In the current study, canopy width and canopy height were identified as good candidate parameters to evaluate the growth performance of rice over the whole life cycle in the cultivars RD41, PT1, Homchonlasit, IR64, Riceberry and RD43. Canopy width, canopy height and leaf area have been used as candidate parameters for identifying the growth status of several plants based on high-throughput phenotyping measurements, such as for rice (Campbell et al., 2015, 2017), maize (Zhang et al., 2017b), *Miscanthus* (Malinowska et al., 2017) and rapeseed (Xiong et al., 2017). Conventional (manual data measurement) and automatic data collection in seven rice cultivars at the early seedling stage, as well as the relationships of those parameters, has been well established (Anandan et al.,

2020). The canopy width and canopy height of the cultivars RD41 and RD43 (early harvest genotypes) showed a compact plant architecture throughout the whole life cycle. Previously, shoot height estimation of 553 landrace and elite accessions of rice at the milk-grain stage compared to the tillering stage was evaluated using RAP (rice automatic phenotyping platform), and the relationships among those data were expressed as linear correlations (Yang et al., 2014). The shoot height and leaf width of bananas estimated using RGB-D sensors (Vit et al., 2019) and the leaf area of soybean estimated using pixels (Zhu et al., 2020) have been successfully validated with high accuracy. A linear relationship of shoot height obtained from conventional measurement versus automatic measurement was also reported for maize (R^2 = 0.98) (Zhang et al., 2017b), rapeseed (R^2 = 0.84) (Xiong et al., 2017) and the genus *Arabidopsis* (R^2 = 0.898; Arend et al., 2016). Data obtained for the plant projected area from manual measurements and RGB estimations were divided into the vegetative stage (seedling and tillering) and the reproductive stage to establish the best model of the relationship. Leaf arrangement and the overlap of leaf position of the whole plant canopy have the lowest effect values for leaf area compared with those determined by the conventional method, which leads to underestimation of the plant projected area (Fanourakis et al., 2014). Canopy architecture is a major factor that reduces the accuracy of estimation of digital plant phenotyping platforms (Liu et al., 2019). A linear relationship between plant green area and actual architectural measurements was observed in eight DAT seedlings of 373 genotypes under treatment with 270 mM NaCl: 9.9 mM $CaCl_2$ for 20 d (R^2 = 0.96; Campbell et al., 2015).

High-throughput plant phenotyping with digital information is indispensable for nondestructive plant growth measurements (Mir et al., 2019). A relationship between the parameters obtained from conventional measurement and those from RGB estimation has been reported. For example, automatic digital measurement of the estimated tiller diameter using CT-RGB phenotyping and actual measurement data in 35 accessions of rice produced an R^2 value of 0.959 (Wu et al., 2019). Plant projected area has been applied to the biomass measurements of plants in terms of FW and DW in several crop species, including the genus *Arabidopsis* (Arend et al., 2016), tomatoes (Laxma et al., 2018), rice (Yang et al., 2014; Kim et al., 2020), maize (Ge et al., 2016) and *Setaria* (Fahlgren et al., 2015a). In two inbred maize genotypes (B73 and FFMM-A), a linear relationship between shoot FW and plant projected area (pixel count) at the early stage (6–26 DAP) was demonstrated with a high R^2 value (0.993). However, the relationships between plant biomass and projected area were very weak when the developmental stage of plants was increased (26-46 DAP; Ge et al., 2016). Laxma et al. (2018) found a linear relationship between shoot FW and projected shoot area with an R^2 value of 0.85 in four tomato cultivars (Arka Rakshak, Arka Samrat, Arka Ashish and Abhinav). In the current study at harvest, the yield of rice was linearly correlated with the shoot DW with a relatively high correlation (R^2 = 0.44). The agronomical traits and yield components of RD41, PT1, Homchonlasit, IR64, Riceberry and RD43 fluctuated depending on early or late harvest times, the stay-green types and their interaction.

Conclusion

The current study validated high-throughput phenotyping of the whole life cycle of the indica rice genotypes RD41, PT1, Homchonlasit, IR64, Riceberry and RD43 based on a comparison with actual measurements. Canopy height, canopy width and leaf area in each developmental stage were related to rice biomass. A close relationship was observed in the vegetative stage between non-destructive estimations and conventional measurements of the number of tillers, canopy width and shoot FW, and plant projected area and shoot DW. These findings suggested that high-throughput phenotype techniques could be used to rapidly assess the growth and biomass of indica rice using non-destructive samples.

Conflict of Interest

The authors declare that there are no conflicts of interest.

Acknowledgments

This work was supported by the National Center for Genetic Engineering and Biotechnology (BIOTEC), National Science and Technology Development Agency (NSTDA), (grant numbers P-18-51456, 2021).

References

Anandan, A., Mahender, A., Sah, R.P., Bose, L.K., Subudhi, H., Meher, J., Reddy, J.N., Ali, J. 2020. Non-destructive phenotyping for early seedling vigor in direct-seeded rice. Plant Met. 16: 127. doi.org/10.1186/s13007-020-00666-6

Araus, J.L., Cairns, J.E. 2014. Field high-throughput phenotyping: The new crop breeding frontier. Trends Plant Sci. 19: 52–61. doi.org/10.1016/j.tplants.2013.09.008

Araus, J.L., Kefauver, S.C., Zaman-Allah, M., Olsen, M.S., Cairns, J.E. 2018. Translating high-throughput phenotyping into genetic gain. Trends Plant Sci. 23: 451–466. doi.org/10.1016/j.tplants.2018.02.001

Arend, D., Lange, M., Pape, J.M., et al. 2016. Quantitative monitoring of *Arabidopsis thaliana* growth and development using high-throughput plant phenotyping. Sci Data. 3: 160055. doi.org/10.1038/sdata.2016.55

Campbell, M.T., Du, Q., Liu, K., Brien, C.J., Berger, B., Zhang, C., Walia, H. 2017. A comprehensive imaged-based phenomics analysis reveals the complex genetic architecture of shoot growth dynamics in rice (*Oryza sativa*). Plant Genome 10: 1–14. doi.org/10.3835/plantgenome2016.07.0064

Campbell, M.T., Knecht, A.C., Berger, B., Brien, C.J., Wang, D., Walia, H. 2015. Integrating image-based phenomics and association analysis to dissect the genetic architecture of temporal salinity responses in rice. Plant Physiol. 168: 1476–1489 doi.org/10.1104/pp.15.00450

Cha-um, S., Kirdmanee, C. 2010. Effect of glycinebetaine on proline, water use, and photosynthetic efficiencies, and growth of rice seedlings under salt stress. Turkish J. Agric. Forest. 34: 517–527. doi:10.3906/tar-0906-34

Chawade, A., Armoniene, R., Berg, G., et al. 2018. A transnational and holistic breeding approach is needed for sustainable wheat production in the Baltic Sea region. Physiol Plant. 164:442–451. doi.org/10.1111/ppl.12726

Chin, H.S., Wu, Y.P., Hour, A.L., Hong, C.Y., Lin, Y.R. 2016. Genetic and evolutionary analysis of purple leaf sheath in rice. Rice9: 8. doi.org/10.1186/s12284-016-0080-y

Daiponmak, W., Theerakulpisut, P., Thanonkao, P., Vanavichit, A., Prathepha, P. 2010. Changes of anthocyanin cyanidin-3-glucoside content and antioxidant activity in Thai rice varieties under salinity stress. ScienceAsia 36: 286–291. doi.org/10.2306/scienceasia1513-1874.2010.36.286

Dhondt, S., Wuyts, N., Inzé, D. 2013. Cell to whole plant phenotyping: The best is yet to come. Trends Plant Sci. 18: 433–444. doi.org/10.1016/j.tplants.2013.04.008

Dingkuhn, M., Laza, M.R.C., Kumar, U., et al. 2015. Improving yield potential of tropical rice: Achieved levels and perspectives through improved ideotypes. Field Crop. Res. 182: 43–59. doi.org/10.1016/j.fcr.2015.05.025

Fahlgren, N., Feldman, M., Gehan, M.A., et al. 2015a. A versatile phenotyping system and analytics platform reveals diverse temporal responses to water availability in *Setaria*. Mol. Plant 8: 1520–1535. doi.org/10.1016/j.molp.2015.06.005

Fahlgren, N., Gehan, M.A., Baxter, I. 2015b. Lights, camera, action: High-throughput plant phenotyping is ready for a close-up. Curr. Opin. Plant Biol. 24: 93–99. doi.org/10.1016/j.pbi.2015.02.006

Fanourakis, D., Briese, C., Max, J.F.J., Kleinen, S., Putz, A., Fiorani, F., Ulbrich, A., Schurr, U. 2014. Rapid determination of leaf area and plant height by using light curtain arrays in four species with contrasting shoot architecture. Plant Methods 10: 9. http://www.plantmethods.com/content/10/1/9

Fiorani, F., Schurr, U. 2013. Future scenarios for plant phenotyping. Annu. Rev. Plant Biol. 64: 267–291. doi.org/10.1146/annurev-arplant-050312-120137

Firdaus, R.R., Tan, M.L., Rahmat, S.R., Gunaratne, S.M. 2020. Paddy, rice and food security in Malaysia: A review of climate change impacts. Cogent Soc. Sci. 6:1818373. doi.org/10.1080/23311886.2020.1818373

Ge, Y., Bai, G., Stoerger, V., Schnable, J.C. 2016. Temporal dynamics of maize plant growth, water use, and leaf water content using automated high throughput RGB and hyperspectral imaging. Comput. Electron. Agr. 127: 625–632. doi.org/10.1016/j.compag.2016.07.028

Großkinsky, D.K., Svensgaard, J., Christensen, S., Roitsch, T. 2015. Plant phenomics and the need for physiological phenotyping across scales to narrow the genotype-to phenotype knowledge gap. J. Exp. Bot. 66: 5429–5440. doi.org/10.1093/jxb/erv345

Haghshenas, H., Soltani, A., Malidarreh, A.G, Norouzi, H.A, Dastan, S. 2020. Selecting the ideotype of improved rice cultivars using multiple regression and multivariate models. Arch. Agron. Soil Sci. 66: 1134–1153. doi.org/10.1080/03650340.2019.1658866

He, Z., Li, S., Wang, Y., Hu, Y., Chen, F. 2019. Assessment of leaf area index of rice for a growing cycle using multi-temporal C-Band PolSAR datasets. Remote Sens. 11: 2640. doi.org/10.3390/rs11222640

Jiang, Y., Li, C. 2020. Convolutional neural networks for image-based high-throughput plant phenotyping: A review. Plant Phenomics 20: 4152816. doi.org/10.34133/2020/4152816

Khan, A., Jalil, S., Cao, H., Tsago, Y., Sunusi, M., Chen, Z., Shi, C., Jin, X. 2020. The purple leaf (*pl6*) mutation regulates leaf color by altering the anthocyanin and chlorophyll contents in rice. Plants 9: 1477. doi.org/10.3390/plants9111477

Khush, G.S. 2005. What it will take to feed 5.0 billion rice consumers in 2030. Plant Mol. Biol. 59: 1–6. doi.org/10.1007/s11103-005-2159-5

Kim, S.L., Kim, N., Lee, H., et al. 2020. High-throughput phenotyping platform for analyzing drought tolerance in rice. Planta. 252: 38. doi.org/10.1007/s00425-020-03436-9

Klukas, C., Chen, D., Pape, J.M. 2014. Integrated analysis platform: An open-source information system for high-throughput plant phenotyping. Plant Physiol. 65: 506–518. doi.org/10.1104/pp.113.233932

Laxma, R.H., Hemamalini, P., Bhatt, R.M., Sadashiva, A.T. 2018. Non-invasive quantification of tomato (*Solanum lycoperscum* L.). Ind. J. Plant Physiol. 23: 369–375. doi.org/10.1007/s40502-018-0374-8

Lee, U., Chang, S., Putra, G.A., Kim, H., Kim, D.H. 2018. An automated, high-throughput plant phenotyping system using machine learning-based plant segmentation and image analysis. PLoS One 13: e0196615. doi.org/10.1371/journal.pone.0196615

Li, L., Zhang, Q., Huang, D. 2014. A review of imaging techniques for plant phenotyping. Sensors 14: 20078–20111. doi.org/10.3390/s141120078

Li, R., Li, M., Ashraf, U., Liu, S., Zhang, J. 2019. Exploring the relationships between yield and yield-related traits for rice varieties released in China from 1978 to 2017. Front. Plant Sci. 10: 543. doi.org/10.3389/fpls.2019.00543

Liang, T., Xu, Z.J., Chen, W.F. 2017. Advances and prospects of super rice breeding in China. J. Integr. Agr. 16: 984–991. doi.org/10.1016/S2095-3119(16)61604-0

Liu, S., Martre, P., Buis, S., Abichou, M., Andrieu, B., Baret, F. 2019. Estimation of plant and canopy architectural traits using the digital plant phenotyping platform. Plant Physiol. 181: 881–890. doi.org/10.1104/pp.19.00554

Mackill, D.J., Khush, G.S. 2018. IR64: A high-quality and high-yielding mega variety. Rice 11: 18. doi.org/10.1186/s12284-018-0208-3

Malinowska, M., Donnison, I.S., Robson, P.R.H. 2017. Phenomics analysis of drought responses in *Macanthus* collected from different geographical locations. GCB Bioenergy 9: 78–91. doi.org/10.1111/gcbb.12350

Mir, R.R., Reynolds, M., Pinto, F., Khan, M.A., Bhat, M.A. 2019. High-throughput phenotyping for crop improvement in the genomics era. Plant Sci. 282: 60–72. doi.org/10.1016/j.plantsci.2019.01.007

Muthayya, S., Sugimoto, J.D., Montgomery, S., Maberly, G.F. 2014. An overview of global rice production, supply, trade, and consumption. Ann. N.Y. Acad. Sci. 1324: 7–14. doi.org/10.1111/nyas.12540

Office of Agricultural Economics. 2021. Agricultural statistics of Thailand 2021. Ministry of Agriculture and Cooperatives, Bangkok, Thailand. [in Thai]

Omari, M.K., Lee, J., Faqeerzada, M.A., Joshi, R., Park, E., Cho, B.K. 2020. Digital image-based plant phenotyping: A review. Korean J. Agric. Sci. 47: 119–130.

Peng, C., Lin, Z., Lin, G., Chen, S. 2006. The anti-photooxidation of anthocyanins-rich leaves of a purple rice cultivar. Sci. China Ser. C. 49: 543–551. doi.org/10.1007/s11427-006-2022-1

Peng, S., Khush, G.S., Virk, P., Tang, Q., Zou, Y. 2008. Progress in ideotype breeding to increase rice yield potential. Field Crop. Res. 108: 32–38. doi.org/10.1016/j.fcr.2008.04.001

Phonsakhan, W., Kong-Ngern, K. 2015. A comparative proteomic study of white and black glutinous rice leaves. Electron. J. Biotechn. 18: 29–34. dx.doi.org/10.1016/j.ejbt.2014.11.005

Pongprayoon, W., Tisarum, R., Theerawittaya, C., Cha-um, S. 2019. Evaluation and clustering on salt-tolerant ability in rice genotypes (*Oryza sativa* L. subsp. *indica*) using multivariate physiological indices. Physiol. Mol. Biol. Plants 25: 473–483. doi.org/10.1007/s12298-018-00636-2

Tisarum, R., Theerawitaya, C., Samphumphung, T., Takabe, T., Cha-um, S. 2019. Exogenous foliar application of glycine betaine to alleviate water deficit tolerance in two *Indica* rice genotypes under greenhouse conditions. Agronomy 9: 138. doi.org/10.3390/agronomy9030138

Vit, A., Shani, G., Bar-Hillel, A. 2019. Length phenotyping with interest point detection. In: Proceedings of the IEEE/CVF Conference on Computer Vision and Pattern Recognition Workshops. CA, USA, pp. 1–10.

Wang, R., Qiu, Y., Zhou, Y., Liang, Z., Schnable, J.C. 2020. A high-throughput phenotyping pipeline for image processing and functional growth curve analysis. Plant Phenomics 2020: 7481687. doi.org/10.34133/2020/7481687

Wu, D., Guo, Z., Ye, J., et al. 2019. Combining high-throughput micro-CT-RGB phenotyping and genome-wide association study to dissect the genetic architecture of tiller growth in rice. J. Exp. Bot. 70: 545–561. doi.org/10.1093/jxb/ery373

Xiong, X., Yu, L., Yang, W., et al. 2017. A high-throughput stereo-imaging system for quantifying rape leaf traits during the seedling stage. Plant Methods 13: 7. doi.org/10.1186/s13007-017-0157-7

Yang, W., Duan, L., Chen, G., Xiong, L., Liu, Q. 2013. Plant phenomics and high-throughput phenotyping: accelerating rice functional genomics using multidisciplinary technologies. Curr. Opin. Plant Biol. 16: 180–187. doi.org/10.1016/j.pbi.2013.03.005

Yang, W., Feng, H., Zhang, X., Zhang, J., Doonan, J.H., Batchelor, W.D., Xiong, L., Yan, J. 2020. Crop phenomics and high-throughput phenotyping: Past decades, current challenges, and future perspectives. Mol. Plant. 13: 187–214. doi.org/10.1016/j.molp.2020.01.008

Yang, W., Guo, Z., Huang, C., et al. 2014. Combining high-throughput phenotyping and genome-wide association studies to reveal natural genetic variation in rice. Nat. Commun. 5: 5087. doi.org/10.1038/ncomms6087

Zhang, S., Hu, J., Yang, C., et al., 2017a. Genotype by environment interactions for grain yield of perennial rice derivatives (*Oryza sativa* L./*Oryza longistaminata*) in southern China and Laos. Field Crop. Res. 207: 62–70. doi.org/10.1016/j.fcr.2017.03.007

Zhang, X., Huang, C., Wu, D., et al. 2017b. High-throughput phenotyping and QTL mapping reveals the genetics architecture of maize plant growth. Plant Physiol. 173: 1554–1564. doi.org/10.1104/pp.16.01516

Zhang, Y., Liu, X.H., Su, S.L., Wang, C.Z. 2014. Retrieving canopy height and density of paddy rice from Radatsat-2 images with a canopy scattering model. Int. J. Appl. Earth Obs. 28: 170–180. doi.org/10.1016/j.jag.2013.12.005

Zheng, H., Cheng, T., Zhou, M., Li, D., Yao, X., Tian, Y., Cao, W., Zhu, Y. 2019. Improved estimation of rice aboveground biomass combining textural and spectral analysis of UAV imagery. Precision Agric. 20: 611–629. doi.org/10.1007/s11119-018-9600-7

Zhu, Y., Zhong, Q., Yang, C., Wang, D., Li, X., Chen, C., Gao, Y. 2020. A quantitative analysis method of soybean leaf based on key point detection. In: 2020 International Conference on Internet of Things and Intelligent Applications. Zhenjiang, China, pp. 1–5. doi.org/10.1109/ITIA50152.2020.9312274